

A Camera Calibration Method with Large Oblique Angle Machine Vision

Meng Chen¹, YueLei He¹, PeiYi Gong², ZaiWei Li¹ and HongYao Lu¹

¹ School of Urban Transportation, Shanghai University of Engineering Science, Shanghai 201620, China

² Shanghai Xintie Mechanical & Electrical Technology co., LTD, Shanghai 201100, China

Meng Chen: cm109544@163.com, YueLei He: hyl doc@163.com

Abstract. In order to ensure the safety of the subway when it stops at the platform, it is necessary to detect the limits of the subway platform. However, the currently used station limit detection tools have large detection errors and low efficiency, and cannot meet the detection requirements. In this paper, a non-contact platform limit detection system based on machine vision is studied, and a new set of comprehensive calibration methods is proposed for the calibration of the camera in the system at large angles. After collecting the images of large multi array points set by camera, the effective calibration area is selected and the reference circle center is extracted from the connected domain and centroid center algorithm. After collecting the images of large multi array points set by camera, the effective calibration area is selected and the reference circle center is extracted from the connected domain and centroid center algorithm. The base circle center is used as the reference point to carry out perspective transformation, and the change matrix is obtained and tested. Finally, the maximum error of pixel calibration is 1.639pixel. It is proved by laboratory and field experiments that the measurement system of this method can obtain the contour geometry of the platform section accurately, and the gauge accuracy is within $\pm 1\text{mm}$ after repeated measurements, and the accuracy of platform height and platform distance can be within $\pm 3\text{mm}$.

1. Introduction

Subway platform clearance is the space required to ensure the safety of vehicles running, stopping and passenger riding in the platform area[1]. Therefore, the penetration limit detection of platform clearance is an important part of metro vehicle outage operation. In recent years, with the rise of machine vision technology, non-contact measurement based on machine vision has gradually replaced the traditional tool measurement in the field of subway limit detection field. In high-precision vision measurement, the accuracy of the system will directly affect the results of the system measurement. Therefore, the calibration of system accuracy is a crucial step in the construction of the system.

At present, the commonly used plane calibration boards are chessboard format [2], black and white format[3], black and white dot array[4]. These calibration plates are regularly distributed with some characteristic points. Among them, there is a classical Zhang Zhengyou calibration method for checkerboard[5]. The use of Harris corner detection to find the relationship between the world coordinates and the image coordinates reduces the complexity of the algorithm, and the calibration plate is easy to produce and has been widely used. However, this method is based on multi-vision



vision and multiple checkerboard images for calibration. It is not suitable for camera calibration based on monocular vision and single image. Because of its advantages of convenient recognition and high positioning accuracy, circular marking points are widely used in the field of stereo vision. At present, there are many methods for extracting the center point of the dot array calibration plate. The literature[6-8] uses the ellipse fitting method to extract and mark the center of the ellipse image; In literature[9], the 3 ellipse boundary information on the calibration plate is searched through the algorithm and the public tangent line of the ellipse is searched to extract the center point. In the above calibration algorithm, the angle between the camera and the target is small, the acquired target image is often not greatly distorted, and the feature points are easy to extract, which is not suitable for camera calibration of the system.

Because of the particularity of the rail platform, the camera of the system is to collect the profile profile from a close range and wide perspective, therefore, when the indoor scene is simulated, the target image of the system camera is distorted greatly. This paper presents a high-angle limit detection camera calibration method. Based on a large-scale multi-array calibration plate, an effective calibration area is selected and preprocessed, and then the center of circle algorithm is used to identify the reference circle in the positioning calibration plate and the center coordinates are extracted. The reference circle feature point transforms the image as a reference point for image transformation to complete camera calibration. Finally, the indoor and outdoor test verification of system accuracy.

2. Calibration model establishment area selection

2.1. Establish a calibration model

According to the triangulation principle, the camera calibration model with large inclination angle can be established, as shown in figure 1. When the camera is calibrated, the structured light band emitted by the laser is in the same cross-section as the large multi-array calibration plate. At the same time, adjusting the light and the various components on the instrument to ensure that the parameters in the acquisition process remain unchanged, so as to ensure the consistency of the calibration board images collected multiple times, to avoid the effects of instrument operation, lighting and other external factors on the system calibration accuracy.

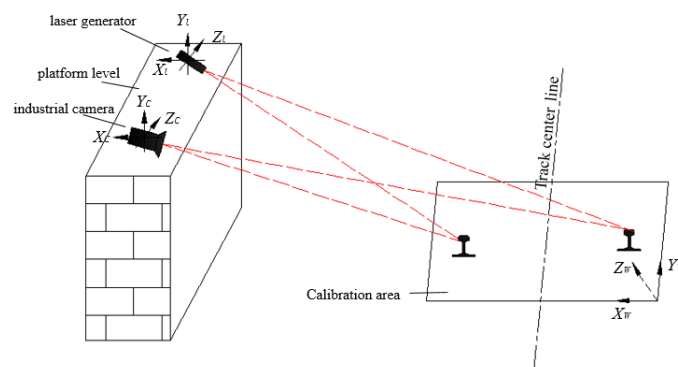


Figure 1. Camera calibration model

2.2 Determine the calibration area

The calibration plate, as shown in figure 2, is shown in Figure 2. The overall size is 2400*2400mm, and the calibration board is square array with 3600 reference circles with a diameter of 20mm. The adjacent base circle center distance is 40mm, and the overall machining precision of the calibration board is more than 0.02mm. In addition, the reference circle is set to black, and the metal background is set to silver-white, so that there is a clear gray difference between the two, and the quality of the divided reference circle is improved.



Figure 2. Calibration plate

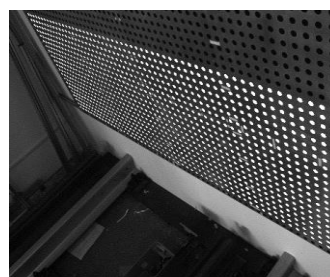


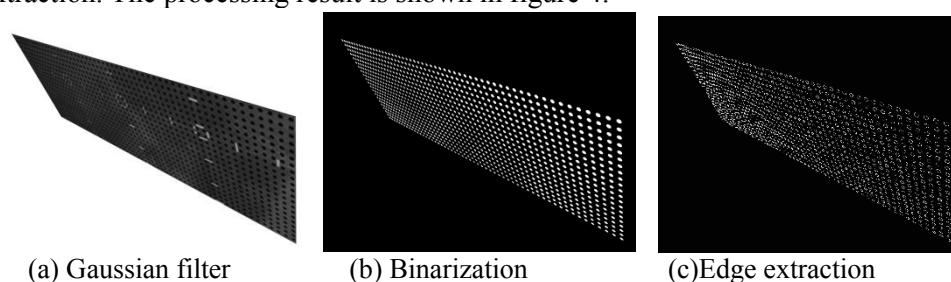
Figure 3. Baseline in the effective calibration area

Determine the effective calibration area based on the station profile actually shot by the system camera as shown in the white reference circle in figure 3. Placing some white interference on the selected calibration plate area to simulate on-site lighting conditions and then image processing. The selection of this area avoids the influence of changes in the edge position on the calibrated pixel accuracy during the calibration of the circle center distance of the reference circle.

3. Reference circle center extraction and image transformation

3.1 demarcated area preprocessing

For the selected calibration area, image preprocessing is first performed using Gaussian filtering [10] for smoothing, then using local thresholding [11] for binarization and finally using Sobel operator [12] for edge extraction. The processing result is shown in figure 4.



(a) Gaussian filter

(b) Binarization

(c) Edge extraction

Figure 4. Image Preprocessing

3.2 Center extraction

The connected area generally refers to an image area consisting of foreground pixel points with the same pixel value and adjacent positions in the image.

Commonly used adjacencies include two kinds: 4 neighborhoods and 8 neighborhoods. 4 neighborhoods for a total of 4 points. If there are pixels, then the four-neighborhood is the top, bottom, left, and right adjacent points of the point. In addition to the four-neighborhood point, the eight-neighborhood includes four diagonal points. Based on the 8-neighborhood labeling algorithm and the centroid localization algorithm, this paper proposes a centroid algorithm and combines the large multi-array calibration plate used to achieve the extraction of the reference circle center. The specific algorithm steps are as follows:

Step1: Read the calibration image after extracting the edges, and traverse the entire image from top to bottom and from left to right.

Step2: Give each pixel a label and assign the same label to the set of pixels in the same connected region.

Step3: The resulting connected area is marked with a circumscribed rectangle until all connected fields are marked.

Step4: Judge whether there is a non-reference circle in the connected area of the marker. If yes, set the connected area size and delete the non-reference circle connected area; if not, enter Step5;

Step5: Based on the principle of graph centroid, the obtained circle-connected circle is marked and encoded by the circle center, and the coordinate data file is output.

Figure 5 is the result of the center of the circle.



(a) Bounding rectangle positioning (b) Center extraction and encoding

Figure 5. The center of circle results

3.3 Image transformation

The large multi-plane plane calibration plate used in this paper establishes a two-dimensional world coordinate system. Set the coordinate point of any point T on the calibration plate as (X, Y) the image coordinate corresponding to the projection is $T'(x, y)$, The coordinate system relationship between the object point and the image point is shown in figure 6.

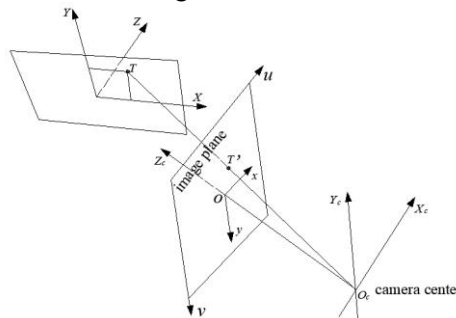


Figure 6. Coordinates of object points and image points

Perspective transformation [13] essentially projects an image onto a new viewing plane. The general formula is:

$$\begin{bmatrix} x & y & z \end{bmatrix} = \begin{bmatrix} X & Y & Z \end{bmatrix} \begin{bmatrix} a_{11} & a_{12} & a_{13} \\ a_{21} & a_{22} & a_{23} \\ a_{31} & a_{32} & a_{33} \end{bmatrix} \quad (1)$$

$z = a_{13}X + a_{23}Y + a_{33}Z$, $[x, y, z]$ is a homogeneous coordinate, the transformed image pixel coordinates are: $\begin{bmatrix} \frac{x}{z} & \frac{y}{z} & 1 \end{bmatrix}$. Transformation matrix $\begin{bmatrix} a_{11} & a_{12} & a_{13} \\ a_{21} & a_{22} & a_{23} \\ a_{31} & a_{32} & a_{33} \end{bmatrix}$ can be split into four parts: $\begin{bmatrix} a_{11} & a_{12} \\ a_{13} & a_{14} \end{bmatrix}$

is used for image linear transformation, $[a_{31} \ a_{32}]$ is used for image translation, $[a_{13} \ a_{23}]^T$ is used to generate an image perspective transformation. The transformed coordinate value (u, v) can be obtained by the following formula:

$$X = \frac{x}{z} = \frac{a_{11}X + a_{21}Y + a_{31}}{a_{13}X + a_{23}Y + a_{33}} \quad (2)$$

$$Y = \frac{y}{z} = \frac{a_{12}X + a_{22}Y + a_{32}}{a_{13}X + a_{23}Y + a_{33}} \quad (3)$$

Selecting the four corner points of the outer circle reference circle in the calibration area: $P_1(x_1, y_1), P_{192}(x_{192}, y_{192}), P_{1158}(x_{1158}, y_{1158}), P_{1176}(x_{1176}, y_{1176})$, the coordinates in the corresponding world coordinate system are: $P_1(x_1, y_1), P_{192}(x_{192}, y_{192}), P_{1158}(x_{1158}, y_{1158}), P_{1176}(x_{1176}, y_{1176})$. According to

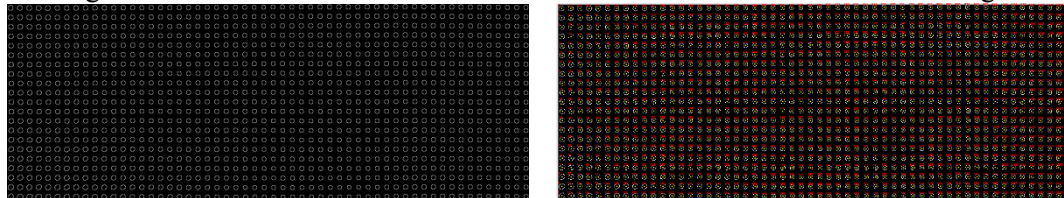
equations (2), (3) and written in a matrix multiplied form:

$$\begin{bmatrix} x_1 & y_1 & 1 & 0 & 0 & 0 & -X_1x_1 & -X_1y_1 \\ 0 & 0 & 0 & x_1 & y_1 & 1 & -Y_1x_1 & -Y_1y_1 \\ x_{192} & y_{192} & 1 & 0 & 0 & 0 & -X_{192}x_{192} & -X_{192}y_{192} \\ 0 & 0 & 0 & x_{192} & y_{192} & 1 & -Y_{192}x_{192} & -Y_{192}y_{192} \\ x_{1158} & y_{1158} & 1 & 0 & 0 & 0 & -X_{1158}x_{1158} & -X_{1158}y_{1158} \\ 0 & 0 & 0 & x_{1158} & y_{1158} & 1 & -Y_{1158}x_{1158} & -Y_{1158}y_{1158} \\ x_{1176} & y_{1176} & 1 & 0 & 0 & 0 & -X_{1176}x_{1176} & -X_{1176}y_{1176} \\ 0 & 0 & 0 & x_{1176} & y_{1176} & 1 & -Y_{1176}x_{1176} & -Y_{1176}y_{1176} \end{bmatrix} \begin{bmatrix} a_{11} \\ a_{21} \\ a_{31} \\ a_{12} \\ a_{22} \\ a_{32} \\ a_{13} \\ a_{23} \end{bmatrix} = \begin{bmatrix} X_1 \\ Y_1 \\ X_{192} \\ Y_{192} \\ X_{1158} \\ Y_{1158} \\ X_{1176} \\ Y_{1176} \end{bmatrix} \quad (4)$$

(4) is marked as: $M * A = Q$, so the transformation matrix is $A = M^{-1} * Q$, According to the above operation steps, an image perspective transformation matrix M is obtained:

$$M = \begin{bmatrix} 1.024 & -0.223 & -35.519 \\ -1.772 & 2.842 & 125.307 \\ -0.001 & 0.001 & 1 \end{bmatrix} \quad (5)$$

The image and center extraction of the transformed calibration board are shown in figure 7.



(a) Calibrated plate image after transformation (b)Center coding

Figure 7. Image results after transformation

4. Experimental verification

The accuracy of the calibration was verified from two aspects. On the one hand, the difference between the theoretical coordinate and the actual coordinate of the center of the reference circle in the transformed calibration board image was used. On the other hand, the system was used to detect the limit indicator of the platform in the field.

4.1 Calibration accuracy verification

The theoretical circle of the reference circle center in the corrected calibration area is recorded as C_i , the actual coordinates are recorded as C'_i , The absolute error value of the two is calculated by Δ_i :

$$\Delta_i = |C_i - C'_i|, \text{ where } i = 1, 2, \dots, 1176 \quad (6)$$

According to the result of equation (6), the absolute difference between the corrected center of the reference circle theory and the actual coordinates can be obtained as shown in figure 8.

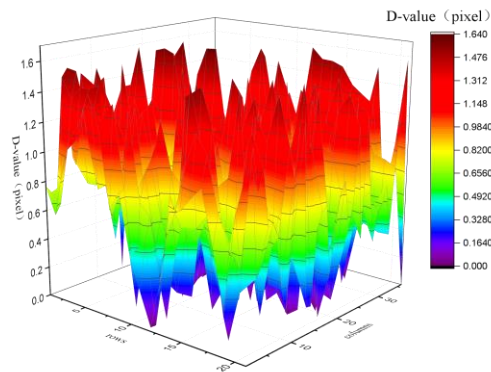


Figure 8. The absolute error distribution of the center coordinates

The maximum absolute coordinate difference is $\Delta_{\max} = 1.639 \text{ pixel}$, the standard deviation is $\sigma = \sqrt{\frac{1}{1176} \sum_{i=1}^{1176} (\Delta_i - \bar{\Delta}_i)^2} = 0.419$ ($\bar{\Delta}_i$ is the difference between the theoretical coordinates of the center of the circle and the actual coordinates). Thus, the calibration accuracy of the system calibration method used in this paper is better.

4.2 Measured data analysis

In order to further verify the robustness and system accuracy of the calibration method in this paper, a field test was conducted at a subway station in Shanghai. figure 9 shows the image of the field test.



Figure 9. System field test

Three geometric dimensions of gauge, platform height (rail top to platform distance) and platform distance (distance between track center line to the edge of rubber strip) are detected. Through the subway station platform detection tool gauge gauge (accuracy $\pm 0.5\text{mm}$), platform ruler (accuracy $\pm 1\text{mm}$) and this system to test 50 platform sections, and compare the detection values and trends, verify the effectiveness of the system data detection.

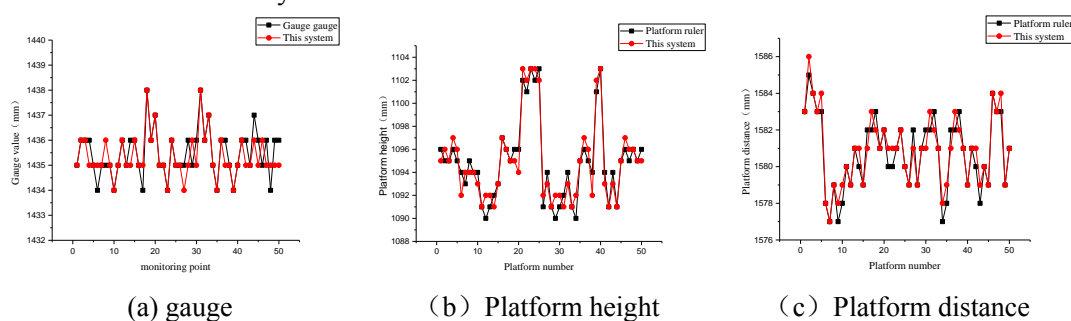


Figure 10. Data analysis (Unit: mm)

From figure 10, it can be seen that the measurement data of the platform meter and the track ruler are basically the same, and the maximum difference is 1mm, which satisfies the requirements of the Urban Rail Transit Engineering Measurement Specification (GB50308-2008). From the test data of platform distance and platform height, it can be seen that the trend of data of platform meter and platform ruler is relatively consistent, the maximum error is below 2mm, and the maximum detection error satisfies the requirements of Metro Design Code (GB50157 - 2013). The data analysis of the above detection results verifies the reliability of calibration accuracy of the calibration method described in this paper, and fully satisfies the requirements for the detection of the limit of the MTR in each life cycle limit.

5. Conclusions

In this paper, a comprehensive calibration method based on large multi array calibration plate is proposed, the key calibration area is selected, and the image preprocessing is carried out by Gauss fuzzy. The domain core method is proposed to segment the reference circle and extract the center of the circle. The feature value is found out according to the center of the circle and the perspective transformation matrix is obtained for image transformation. Through repeated experimental tests and field test analysis, it is concluded that the calibration method of this paper has high robustness, the maximum pixel error is 1.639pixel and in the field test, the track gauge detection accuracy can reach

within $\pm 1\text{mm}$, the platform distance and the platform The height is within $\pm 3\text{mm}$, meeting the specification measurement requirements. In addition, unlike the traditional testing tools, the instrument is portable and detachable. At the same time, the operator does not have to enter the platform rail line operation, and the measuring speed is fast, the accuracy and safety are high, and it can meet the time and precision requirements of the subway outage operation.

References

- [1] Feng Wang, HuiLin Yu and XiaoHua Zhao, et al. Discussion on subway station platform clearance [J]. *railway standard design*, 2009, (2): 81-82.
- [2] HaiTao Niu, XunJie Zhao. A new camera calibration method using checkerboard template [J]. *infrared and laser engineering*, 2011, (01): 133-137.
- [3] HaiGang Meng. Improvement of CCD camera calibration method based on plane constraint [D]. *Jilin University*, 2009.
- [4] FanLu Wu, JianJun Liu , Xin Ren and ChunLai Li. Calibration method of deep space exploration panoramic camera based on circular landmarks[J]. *Acta Optica Sinica*, 2013,(11): 147-153.
- [5] Ying Lu, HuiQin Wang, Wei Ju and JunJie Li.Camera calibration algorithm based on Harris-Zhang Zhengyou plane calibration method[J]. *Journal of Xi'an University Of Architecture And Technology (NATURAL SCIENCE EDITION)*,2014,46(06):860-864+870.
- [6] Andrew Fitzgibbon, Maurizio Pilu and Robert B Fisher. Direct least square fitting of ellipses[J]. *IEEE Transaction on Pattern Analysis and Machine Intelligence*, 1999, 21 (5): 476-480.
- [7] Qiao Yu, S. H. Ong. Arc-based evaluation and detection of ellipses[J]. *Pattern Recognition*, 2007, 40 (7): 1990-2003.
- [8] RuiXue Xia, RongSheng Lu, Ning Liu and JingTao Dong. Automatic extraction of feature point coordinates based on dot array targets[J]. *China Mechanical Engineering*, 2010,(16): 1906-1910.
- [9] Peng Xu, JianYe Wang and YanRu Wang. Accurate calculation of coordinates of target center point in camera calibration[J]. *Infrared and Laser Engineering*, 2011,(07): 1342-1346.
- [10] YaoGui Wang. Image Gauss smoothing filter analysis [J]. *Computer and information technology*, 2008 (08): 79-81+90.
- [11] LiangLiang Wang, Li Wang, XiaoRong Gao and ZeYong Wang.Two improved local threshold segmentation algorithms[J].*Modern Electronic Technique*,2009,32(14):78-80.
- [12] ChunJian Hua, XueMei Xiong and Ying Chen.Feature extraction of circular arc profile based on sobel operator[J].*Laser & Optoelectronics Progress*,2018,55(02):239-246.
- [13] LiGang Li, Bo Liu, HongJian You, HaiLiang Peng and YiJun Wu.Analysis and comparison of geometric precision correction algorithms for spaceborne remote sensing images[J].*Acta Photonica Sinica*,2006(07):1028-1034.